To Tilt Your Head or Not To: Potentially

Bijoy K. Ghosh and Indika Wijayasinghe

Abstract— **In this paper we study the human head movement, when the head shifts its orientation between two possible heading directions, as a simple mechanical control system. Head movements obey Donders' constraint (as opposed to the Listing's constraint for eye movement), which states that the allowed orientations of the head are obtained by rotating a fixed 'primary heading direction' by a subclass of rotation matrices. These rotation matrices have their axes of rotation restricted to a fixed surface, called the Donders' surface. Donders' Law states that when head moves spontaneously from left to right and back or from top to bottom and back, the head rotation matrix has no torsional component. On the other hand, when the head moves diagonally from the top left to the bottom right and back or from the top right to the bottom left and back, spontaneously, the axis of rotation has a small torsional component. The torsional component effectively rotates the head with respect to the frontal line of 'heading'. The head appears slightly tilted as a result of the slight torsion. Defining a suitable Riemannian metric, we study dynamic control of head movement when the head orientations satisfy the Donders' constraint throughout its entire trajectory. Head movements are actuated by choosing a suitable potential function and the oscillations are damped by adding a suitable damping term. An important result of this paper is to show the effect of the torsional component as head is allowed to move between two 'headings'. We show that when the peak value of the allowable torsion is high, i.e. when the head is allowed to be more tilted, transition time between two headings is shortened.**

I. INTRODUCTION

Modeling and control of the eye and the head have been the research goals among neurologists, physiologists and engineers since 1845. Notable studies were conducted by Listing [15], Donders [8] and Helmholtz [12] and they showed that the orientations of the eye and the head are restricted to be a function of the gaze and the heading directions, respectively. With the exception of occasional deviation, the eye follows what is known as the **Listing's Law** and likewise the head follows a generalization of the Listing's Law that goes by the name **Donders' Law.**

Eye movement and subsequently the head movement problem had found a renewed interest towards the later part of the 20^{th} century [17], [22], [24] and [28]. Previous studies which used modeling as a means of understanding the control of eye movements, have adopted two main approaches. One focusing on the details of the properties of the EOMs [16], [18] and the other focusing on the control mechanisms using oversimplified linear models with all the details of the above EOM properties ignored but focusing on the information processing and control aspects [21], [23]. In spite of several notable studies of three dimensional eye movements [3], [11] and many others, with the exception of some recent papers in the subject [20], [29], there has not been a rigorous treatment of the topic in the framework of modern control theory and geometric mechanics. Assuming the eye to be a rigid sphere, the problem of eye movement can be treated as a mechanical control system [5], [19] and the results of classical mechanics can be applied [9], [10]. We continue to apply the same approach to the head movement problem by assuming the head to be a perfect sphere and extend the approach presented in [9], [10].

Most of the earlier studies in eye movement have assumed that the head remained fixed and the eye is allowed to move freely. It has been observed by Listing (see [27]), that in this situation the orientation of the eye is completely determined by its gaze direction. Subsequently it has been shown that starting from a frontal gaze, any other gaze direction is obtained by a rotation matrix whose axis of rotation is constrained to lie on a plane, called the Listing's Plane. Consequently, the set of all orientations the eye can assume is a submanifold of $\mathbf{SO}(3)$ (see Boothby [4] for a definition) called **LIST**. Listing has shown that in a head fixed environment, eye orientations are restricted to this specific submanifold **LIST** (see [20], [10]).

In this paper, we are interested in the study of head movement as the head moves spontaneously towards an object following a Listing like constraint that goes by the name Donders' constraint [17], [22] and [28]. Donders' law states that starting from a frontal head position, any other head orientation is obtained by a rotation matrix whose axis of rotation is constrained to lie on a two dimensional surface, called the Donders' Surface [28]. Consequently, the set of all orientations the head can assume spontaneously is a submanifold of $\mathbf{SO}(3)$ called **DOND**. We would like to remark that unlike the eye, head can be oriented voluntarily outside the submanifold **DOND**. For simplicity, we shall not detail this voluntary action in this paper.

As a final remark we note that, simultaneous movement of the eye and the head to fixate on a target, either stationary or moving, is a subject of intense research (see [6], [7], [13])

This material is based upon work supported in part by the National Science Foundation under Grant No. 0523983. Any opinions, findings, and conclusions or recommendations expressed in this material are those of the author(s) and do not necessarily reflect the views of the National Science Foundation.

B. K. Ghosh is the Director of the Laboratory for BioCybernetics and Intelligent Systems, Texas Tech University, Lubbock, Texas, USA bijoy.ghosh@ttu.edu

I. B. Wijayasinghe is a graduate student in the Laboratory for BioCybernetics and Intelligent Systems, Texas Tech University, Lubbock, Texas, USA indika.wijayasinghe@ttu.edu

ISBN 978-963-311-370-7

in recent years. In order to stabilize a target on the retina in the presence of a head movement, the eyes are controlled by the vestibulo-ocular (VOR) reflex [2], [14]. Coordination and control of the eye and the head is a subject of future research.

II. QUATERNIONIC REPRESENTATIONS

Representation of 'eye orientation' using quaternion has already been described in [20]. Likewise, the head orientations can also be described using quaternions. For the sake of clarity, we revisit some of the main ideas in this section. A quaternion is a four tuple of real numbers denoted by Q. We write each element $a \in Q$ as

$$a = a_0\, 1 + a_1\, i + a_2\, j + a_3\, k, \tag{1}$$

and call $a_1\, i + a_2\, j + a_3\, k$ its vector part and $a_0\, 1$ its scalar part. The vector part is identified with the vector (a_1, a_2, a_3) and the scalar part is written simply as a_0. It is natural to define the map

$$vec\ :\ Q\ \rightarrow\ \mathbf{R}^3, \text{ where } a\ \mapsto\ (a_1, a_2, a_3). \tag{2}$$

The space of unit quaternion is identified with the unit sphere in $\mathbf{R}^4$ and denoted by S^3. Each $q \in S^3$ can be written as

$$q = \cos\frac{\phi}{2}\, 1 + \sin\frac{\phi}{2}\, n_1\, i + \sin\frac{\phi}{2}\, n_2\, j + \sin\frac{\phi}{2}\, n_3\, k, \tag{3}$$

where $\phi \in [0, 2\pi]$, and $n = (n_1, n_2, n_3)$ is a unit vector in $\mathbf{R}^3$. If q is an unit quaternion represented as in (3), one can show the following using simple properties of quaternion multiplication –

"The vector $vec[q \bullet (v_1\, i + v_2\, j + v_3\, k) \bullet q^{-1}]$ **is rotation of the vector** (v_1, v_2, v_3) **around the axis** n **by a counterclockwise angle** ϕ**."**

If S^3 is the space of unit quaternions, we define a map between S^3 and $SO(3)$ described as follows

$$rot\ :\ S^3\ \rightarrow\ SO(3) \tag{4}$$

where

$$q = \begin{pmatrix} q_0 \\ q_1 \\ q_2 \\ q_3 \end{pmatrix} \longmapsto \begin{pmatrix} q_0^2+q_1^2-q_2^2-q_3^2 & 2(q_1q_2-q_0q_3) & 2(q_1q_3+q_0q_2) \\ 2(q_1q_2+q_0q_3) & q_0^2+q_2^2-q_1^2-q_3^2 & 2(q_2q_3-q_0q_1) \\ 2(q_1q_3-q_0q_2) & 2(q_2q_3+q_0q_1) & q_0^2+q_3^2-q_1^2-q_2^2 \end{pmatrix}. \tag{5}$$

Recall that $SO(3)$ is the space of all 3×3 matrices W such that $WW^T = I$, the identity matrix and $det\, W = 1$. It can be verified, perhaps not so easily, that for any nonzero vector v in $\mathbf{R}^3$ we have

$$rot(q)\, v\ =\ vec[q \bullet v \bullet q^{-1}],$$

where the symbol $\bullet$ denotes quaternion multiplication. Note that the map 'rot' in (4) is surjective but not $1-1$. This is because both q and $-q$ in S^3 has the same image. We now write down a parametrization of the unit vector 'n' in (3) as

$$n = \begin{pmatrix} \cos\theta\, \cos\alpha \\ \sin\theta\, \cos\alpha \\ \sin\alpha \end{pmatrix}. \tag{6}$$

Combining (3) and (6), we have the following parametrization of unit quaternions

$$q = \begin{pmatrix} \cos\frac{\phi}{2} \\ \sin\frac{\phi}{2}\cos\theta\, \cos\alpha \\ \sin\frac{\phi}{2}\sin\theta\, \cos\alpha \\ \sin\frac{\phi}{2}\sin\alpha \end{pmatrix}. \tag{7}$$

Using the coordinates (θ, ϕ, α) we have the following sequence of maps

$$[0,\pi] \times [0, 2\pi] \times [-\frac{\pi}{2}, \frac{\pi}{2}] \xrightarrow{\rho} S^3 \xrightarrow{rot} SO(3) \xrightarrow{proj} S^2, \tag{8}$$

where

$$\rho((\theta, \phi, \alpha))\ =\ q\ \text{(in (7))},$$

$$rot(q)\ =\ W$$

and

$$proj(W) = \begin{pmatrix} \sin\theta\, \sin\phi\, \cos\alpha\, +\, \cos\theta\, \sin^2\frac{\phi}{2}\, \sin 2\alpha \\ -\cos\theta\, \sin\phi\, \cos\alpha\, +\, \sin\theta\, \sin^2\frac{\phi}{2}\, \sin 2\alpha \\ \cos^2\frac{\phi}{2}\, -\, \sin^2\frac{\phi}{2}\, \cos 2\alpha \end{pmatrix}. \tag{9}$$

The matrix W in $SO(3)$ can be easily written from (5) and has been omitted. The points in S^2 described by (9) provide a description of the head directions as a function of the coordinate angles θ, ϕ, α with respect to an initial head direction of $(0,0,1)^T$, i.e. obtained by rotating the vector $(0,0,1)^T$ using the rotation matrix W.

III. HEAD ORIENTATIONS SATISFYING DONDERS' CONSTRAINT

Donders' law asserts that the axis of rotation 'n' in (6) is restricted to a surface. We shall describe this surface by restricting

$$\alpha\ =\ \varepsilon\, \sin(2\theta) \tag{10}$$

and obtain the axis of rotation as

$$n\ =\ (\cos\theta\, \cos(\varepsilon\, \sin(2\theta)),\, \sin\theta\, \cos(\varepsilon\, \sin(2\theta)),\, \sin(\varepsilon\, \sin(2\theta)))^T,$$

and the unit quaternion vector as

$$q\ =\ (\cos\frac{\phi}{2},\, \sin\frac{\phi}{2}\, \cos\theta\, \cos\alpha,\, \sin\frac{\phi}{2}\, \sin\theta\, \cos\alpha,\, \sin\frac{\phi}{2}\, \sin\alpha)^T.$$

The choice of (10) as a description of the Donders' surface is dictated by the following observation made in [29]

"When the axis of rotation is horizontal or vertical (i.e. when θ is a multiple of $\frac{\pi}{2}$), head moves without any torsion. At other angles of rotation, there is a gradual increase in torsion".

Under the Donders' constraint, we define **DOND** to be the associated submanifold of $\mathbf{S}^3$ and $\mathbf{SO}_D(3)$ to be the associated submanifold of **SO(3)**. They are both two dimensional submanifolds parameterizing the rotation in $\mathbf{S}^3$ and $\mathbf{SO}(3)$ respectively. The heading direction $(0,\,0,\,1)^T$ is transformed to the direction

$$\begin{pmatrix} \sin\theta\,\sin\phi\,\cos(\varepsilon\sin(2\theta)) + \cos\theta\,\sin^2\frac{\phi}{2}\,\sin(2\varepsilon\sin(2\theta)) \\ -\cos\theta\,\sin\phi\,\cos(\varepsilon\sin(2\theta)) + \sin\theta\,\sin^2\frac{\phi}{2}\,\sin(2\varepsilon\sin(2\theta)) \\ \cos^2\frac{\phi}{2} - \sin^2\frac{\phi}{2}\,\cos(2\varepsilon\sin(2\theta)) \end{pmatrix}, \quad (11)$$

by the rotation matrix W.

Donders' constraint is a restriction on the axis of rotation, for head transitions away from the primary head direction, which we assume to be 'looking straight horizontally'. It can be easily checked that the submanifold $\mathbf{SO}_D(3)$ is not a subgroup of **SO(3)** and hence matrix product of two elements of $\mathbf{SO}_D(3)$ would not necessarily be an element of $\mathbf{SO}_D(3)$. What this means is that *head transition between a secondary position and a tertiary position, i.e. away from the primary position,* is not necessarily taking place with an axis of rotation on the Donders' surface.

During transition between two arbitrary head directions, Donders' law is to be viewed as a constraint on the instantaneous orientations of the head, described by the columns of the matrix W. In particular, the orientations are restricted to remain inside $\mathbf{SO}_D(3)$ at all times.

IV. RIEMANNIAN METRIC ON SO(3) AND DOND

It has been described in [20] that eye rotations are typically confined to a sub manifold **LIST** of $\mathbf{SO}(3)$ especially when the head is restrained to be fixed. Likewise, spontaneous head movements are typically confined to a sub manifold **DOND** of $\mathbf{SO}(3)$. In order to write down the equations of motion, one needs to know the kinetic and the potential energies of the eye in motion. The kinetic energy is given by the induced Riemannian metric on **DOND**, induced from the Riemannian metric on $\mathbf{SO}(3)$.

The Riemannian metric is derived by assuming that the head is a perfect sphere and its inertia tensor is equal to the identity matrix $I_{3\times 3}$. This is associated with a left invariant Riemannian metric on $\mathbf{SO}(3)$ given by

$$< \Omega(e_i), \Omega(e_j) >_I = \delta_{i,j}, \quad (12)$$

where

$$\Omega(e_k) = \begin{pmatrix} 0 & \delta_{3,k} & -\delta_{2,k} \\ -\delta_{3,k} & 0 & \delta_{1,k} \\ \delta_{2,k} & -\delta_{1,k} & 0 \end{pmatrix} \quad (13)$$

and $\delta_{l,m}$ denotes the Kronecker delta function. An easy way to carry out computation using this Riemannian metric is provided by an isometric submersion **rot** between $\mathbf{S}^3$ and $\mathbf{SO}(3)$ already described in (4) and (8).

The composition mapping $\mathbf{rot}\circ\rho(\theta,\phi,\alpha)$ is a rotation around the axis (6) by a counterclockwise angle ϕ. In order to compute the Riemannian Metric on $\mathbf{SO}(3)$, we write

$$\rho_*\left(\frac{\partial}{\partial\theta}\right) = \begin{pmatrix} 0 \\ -\sin(\phi/2)\;\sin(\theta)\;\cos(\alpha) \\ \sin(\phi/2)\;\cos(\theta)\;\cos(\alpha) \\ 0 \end{pmatrix}; \quad (14)$$

$$\rho_*\left(\frac{\partial}{\partial\alpha}\right) = \begin{pmatrix} 0 \\ -\sin(\phi/2)\;\cos(\theta)\;\sin(\alpha) \\ -\sin(\phi/2)\;\sin(\theta)\;\sin(\alpha) \\ \sin(\phi/2)\;\cos(\alpha) \end{pmatrix}; \quad (15)$$

$$\rho_*\left(\frac{\partial}{\partial\phi}\right) = \begin{pmatrix} -\frac{1}{2}\sin(\phi/2) \\ \frac{1}{2}\cos(\phi/2)\;\cos(\theta)\;\cos(\alpha) \\ \frac{1}{2}\cos(\phi/2)\;\sin(\theta)\;\cos(\alpha) \\ \frac{1}{2}\cos(\phi/2)\;\sin(\alpha) \end{pmatrix}. \quad (16)$$

Then we obtain the inner products given by,

$$\begin{aligned} g_{11} &= \langle\frac{\partial}{\partial\theta},\frac{\partial}{\partial\theta}\rangle = \sin^2(\phi/2)\cos^2(\alpha) \\ g_{22} &= \langle\frac{\partial}{\partial\alpha},\frac{\partial}{\partial\alpha}\rangle = \sin^2(\phi/2) \\ g_{33} &= \langle\frac{\partial}{\partial\phi},\frac{\partial}{\partial\phi}\rangle = \frac{1}{4} \\ \text{and } g_{ij} &= 0 \text{ for } i\neq j \text{ with } i,j=1,2,3. \end{aligned} \quad (17)$$

The Riemannian metric on $\mathbf{SO}(3)$ is given by:

$$g = \sin^2(\phi/2)\cos^2(\alpha)\,d\theta^2 + \sin^2(\phi/2)\,d\alpha^2 + \frac{1}{4}d\phi^2. \quad (18)$$

Note that restricted to the Donders' surface, i.e. when (10) is satisfied, in order to compute the Riemannian metric on **DOND**, we write

$$\rho_*\left(\frac{\partial}{\partial\theta}\right) = \begin{pmatrix} 0 \\ -\sin(\phi/2)\;\sin(\theta)\;\cos(\alpha) - \sin(\phi/2)\;\cos(\theta)\;\sin(\alpha)\;\frac{\partial\alpha}{\partial\theta} \\ +\sin(\phi/2)\;\cos(\theta)\;\cos(\alpha) - \sin(\phi/2)\;\sin(\theta)\;\sin(\alpha)\;\frac{\partial\alpha}{\partial\theta} \\ \sin(\phi/2)\;\cos(\alpha)\;\frac{\partial\alpha}{\partial\theta} \end{pmatrix}; \quad (19)$$

$$\rho_*\left(\frac{\partial}{\partial\phi}\right) = \begin{pmatrix} -\frac{1}{2}\sin(\phi/2) \\ \frac{1}{2}\cos(\phi/2)\;\cos(\theta)\;\cos(\alpha) \\ \frac{1}{2}\cos(\phi/2)\;\sin(\theta)\;\cos(\alpha) \\ \frac{1}{2}\cos(\phi/2)\;\sin(\alpha) \end{pmatrix}. \quad (20)$$

The Riemannian metric on **DOND** is given by

$$g = \sin^2(\phi/2)\left[\cos^2\alpha + \left(\frac{\partial\alpha}{\partial\theta}\right)^2\right]d\theta^2 + \frac{1}{4}d\phi^2. \quad (21)$$

Using the Riemannian metric (18) for $\mathbf{SO}(3)$, it is a straightforward but tedious computation to show that the associated geodesic equation is given by

$$\begin{aligned} \ddot\theta + \dot\theta\dot\phi\cot(\phi/2) - 2\dot\theta\dot\alpha\tan(\alpha) &= 0 \\ \ddot\phi - (\dot\theta)^2\sin(\phi)\cos^2(\alpha) - (\dot\alpha)^2\sin(\phi) &= 0 \\ \ddot\alpha + \frac{1}{2}(\dot\theta)^2\sin(2\alpha) + \dot\phi\dot\alpha\cot(\phi/2) &= 0. \end{aligned} \quad (22)$$

Using the Riemannian metric (21), the above geodesic equation (22) reduces to the pair of equations

$$\begin{aligned}
&\frac{d}{dt}\left[\sin^2\frac{\phi}{2}\left(\cos^2\alpha+\left(\frac{\partial\alpha}{\partial\theta}\right)^2\right)\dot{\theta}\right]\\
&-\sin^2\frac{\phi}{2}\,\dot{\theta}^2\,\frac{\partial\alpha}{\partial\theta}\left[\frac{\partial^2\alpha}{\partial\theta^2}-\frac{1}{2}\sin(2\alpha)\right] \;=\; 0\\
&\ddot{\phi}-\left[\cos^2\alpha+\left(\frac{\partial\alpha}{\partial\theta}\right)^2\right]\dot{\theta}^2\sin\phi \;=\; 0. \quad (23)
\end{aligned}$$

V. GENERAL EQUATION OF MOTION ON THE DONDERS' SUBMANIFOLD

The Riemannian Metrics that we had obtained so far in (18) and (21) enables us to write down an expression for the kinetic energy KE given by

$$KE \;=\; \frac{1}{2}[\sin^2(\phi/2)\,[\cos^2\alpha \;+\; (\frac{\partial\alpha}{\partial\theta})^2]\dot{\theta}^2+\frac{1}{4}\dot{\phi}^2].$$

In general, the dynamics is affected by an additional potential energy and an external input torque. Let us consider a general form of the potential function given by

$$V(\theta,\phi) \;=\; A\,\sin^2\frac{\phi}{2}\;+\;B\,\sin^2\frac{\theta}{2}, \qquad (24)$$

where $\alpha = \varepsilon\sin(2\theta)$. The expression for the Lagrangian is given by

$$L \;=\; KE \;-\; V, \qquad (25)$$

and the equation of motion is described by

$$\frac{d}{dt}\left(\frac{\partial L}{\partial\dot{\beta}}\right)-\left(\frac{\partial L}{\partial\beta}\right) \;=\; \tau_\beta \qquad (26)$$

where β is the angle variable. The Euler Lagrange's equation on **DOND** is given by

$$\begin{aligned}
&\frac{d}{dt}\left[\sin^2\frac{\phi}{2}\left(\cos^2\alpha+\left(\frac{\partial\alpha}{\partial\theta}\right)^2\right)\dot{\theta}\right]\\
&-\sin^2\frac{\phi}{2}\,\dot{\theta}^2\,\frac{\partial\alpha}{\partial\theta}\left[\frac{\partial^2\alpha}{\partial\theta^2}-\frac{1}{2}\sin(2\alpha)\right] \;=\; -\frac{1}{2}B\sin\theta\;+\;\tau_\theta,\\
&\ddot{\phi}-\left[\cos^2\alpha+\left(\frac{\partial\alpha}{\partial\theta}\right)^2\right]\dot{\theta}^2\sin\phi = -2A\sin\phi\;+\;4\tau_\phi, \qquad (27)
\end{aligned}$$

where, as before, we continue to assume that α satisfies the Donders' constraint (10).

VI. SOME SIMULATIONS ON GEODESIC AND MOTION EQUATION

In this section we show via simulation, some of the geodesic trajectories and solutions to the motion equation under a suitable choice of potential energy and the input torque.

Example 1 (Geodesic Curves): In this example we solve the geodesic equation (23) (corresponds to head rotation that satisfy the Donders' constraint). In Fig. 1 we have plotted the head directions as a function of time starting from one suitably chosen initial condition. In plotting the figure, we have chosen the convention that the identity rotation matrix corresponds to the frontal heading. Our simulation shows that the projection of the geodesic curve on $\mathbf{SO}(2)$ is not periodic.

Example 2 (Motion Equation with a Potential Function and no Damping): In this example we solve the motion equation (27) (corresponds to head movement that satisfy the Donders' constraint) and show the gaze trajectories in Fig. 2. We have assumed $\tau_\theta = \tau_\phi = 0$, and increasing magnitudes A (assuming $B = 0$) of the potential function, in (24), has been chosen. The parameter $\varepsilon = 0.1$. Our simulations show that with increasing magnitude of the parameter A, the gaze trajectories are restricted to a smaller neighborhood of $\phi = 0$, the frontal gaze.

Example 3 (Regulation using a Potential Function and Damping): The problem of **Regulation** is to control the state towards a specific final point, without paying any attention to the intermediate trajectory. This class of problem is of the same kind as was considered for optimal control except that we are not optimizing a cost function. In this example, we show via simulation that by choosing a potential function that has a suitable minimum at the final point of interest, and by choosing a control that simulates the effect of 'damping', we are able to regulate the final position of the state.

We remark that in example 2, one of the properties of the head movement trajectory is that with increasing magnitude A (assuming $B = 0$) of the potential function (24), the head trajectories are restricted to the frontal part of the visual field, a desirable feature. Unfortunately, we observe that the trajectories themselves are increasingly jittery. In this example we repeat example 2 but choose $\tau_\theta = -.1\,\dot{\theta}$ and $\tau_\phi = -.1\,\dot{\phi}$ in (27), in order to dampen the fluctuations in the trajectories. The parameter $\varepsilon = 0.1$ and the results are plotted in Fig. 3. We observe that the state settles down to the point of minimum potential.

Example 4 (Regulation to an arbitrary final point using a Potential Function and Damping): In this example we repeat example 3 and choose $\tau_\theta = -1\,\dot{\theta}$ and $\tau_\phi = -1\,\dot{\phi}$ in (27), in order to dampen the fluctuations in the trajectories. The potential function has a minimum at an arbitrary final gaze direction (given by θ_f, ϕ_f), away from the frontal gaze. This is achieved by modifying the potential function (24) to

$$V(\theta,\phi) \;=\; A\,\left[\sin^2\frac{\phi-\phi_f}{2}\right]\;+\;B\,\left[\sin^2\frac{\theta-\theta_f}{2}\right]. \qquad (28)$$

The results are plotted in Fig. 4, assuming $A = B$. The plots are quite similar to that of Fig. 3 except that the terminal points are different. The final value of θ in Fig. 3 is unconstrained whereas it is constrained in Fig. 4. Note that the final orientation of the head has a non-zero torsional component given by $\alpha = \varepsilon\sin(2\theta_f)$, where $\varepsilon = .1$

Example 5 (How Donders' constraint affect TIME and DISTANCE): In Fig. 5, we have sketched the head movements between two specific directions, that are kept fixed for this example. In Fig. 5a, head movements are shown for

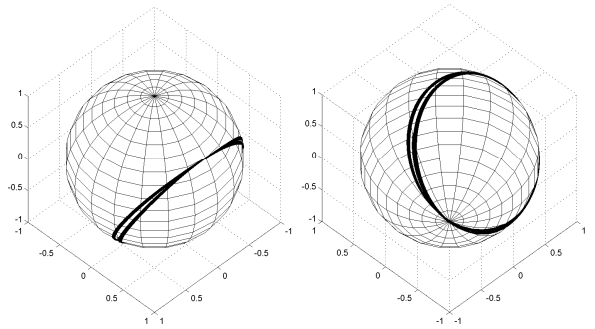

(a) ε = 0.05, Front view (b) ε = 0.1, Back view

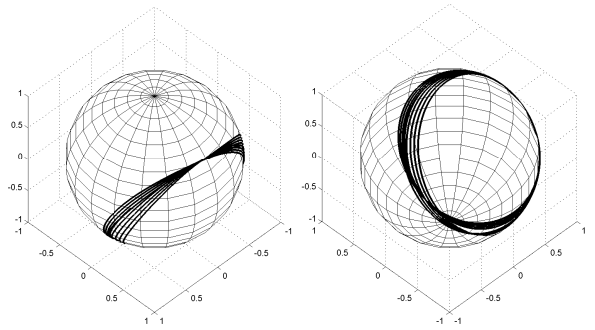

(c) ε = 0.2, Front view (d) ε = 0.3, Back view

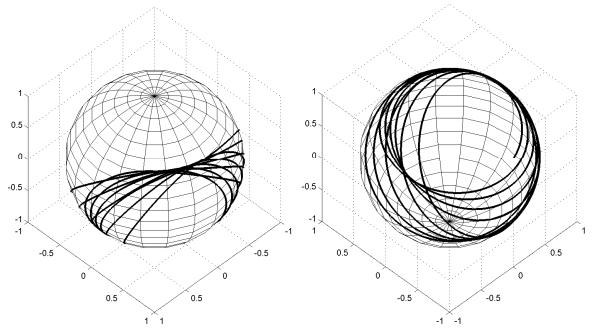

(e) ε = 0.05, Front view (f) ε = 0.1, Back view

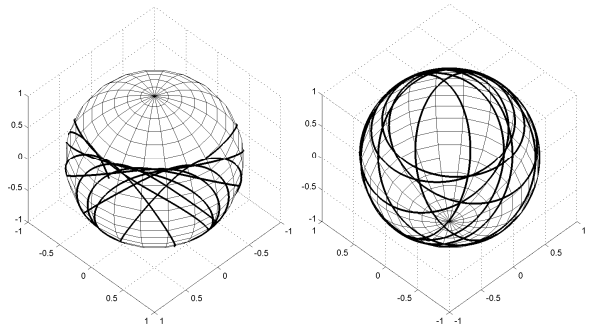

(g) ε = 0.2, Front view (h) ε = 0.3, Back view

Fig. 1: Geodesics for equation (23) for head movement that satisfies Donders' Law. In each of the figures the north pole is the frontal position of the head (left four figures), and the south pole is the backward head position (right four figures). The values of ε, that describe Donders' Law in (10), are given by 0.05, 0.1, 0.2 and 0.3 from top to bottom. The value of $\varepsilon = 0$, not shown in these figures, corresponds to the geodesic for eye movement that satisfies Listing's Law (see [9], [20]).

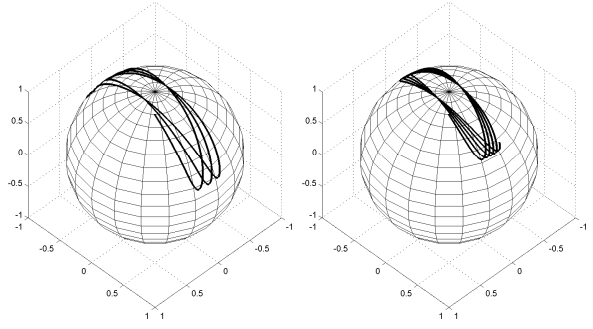

(a) A = 0.5 (b) A = 1

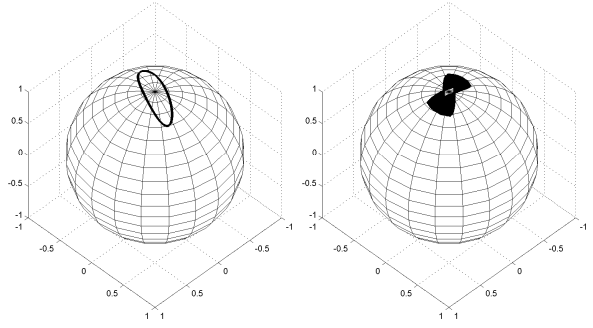

(c) A = 5 (d) A = 50

Fig. 2: Head motion from (27) with the external control set to zero, i.e. $\tau_\theta = \tau_\phi = 0$, $\varepsilon = 0.1$. Increasing magnitude A of the potential function shows that the Head movements are restricted to the frontal head direction.

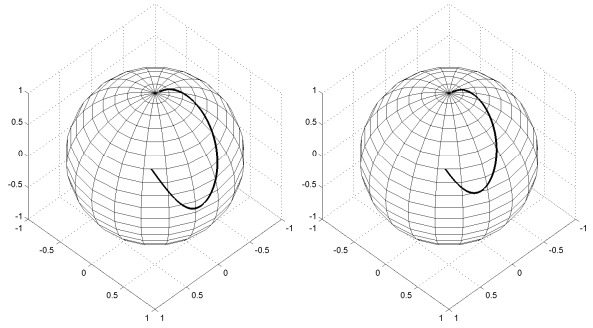

(a) A = 0.5 (b) A = 1

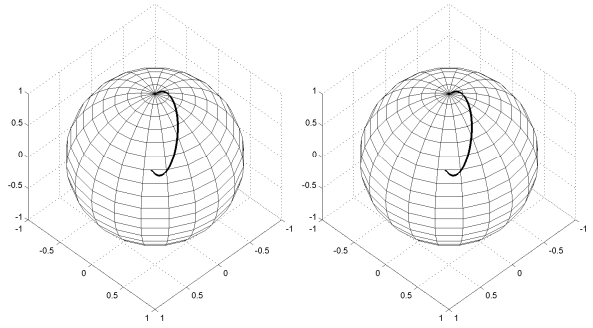

(c) A = 5 (d) A = 50

Fig. 3: Head movement to the frontal head position, under the influence of a potential function and a constant friction term. We have chosen $k = 0.1$ and $\varepsilon = 0.1$.

different values of ε (see definition of Donders' constraint (10)). Although the paths appear to follow similar profile, in Fig. 5b we show that the total distance, computed using the Riemannian metric (21), increases with increasing values of ε. This is understandable since there is an extra head rotation for the same head direction. We also make a surprising observation in Fig. 5b that the time to complete the trajectories fall, as a function of ε, indicating that perhaps *the head is able to move rapidly a larger distance in a shorter time.*

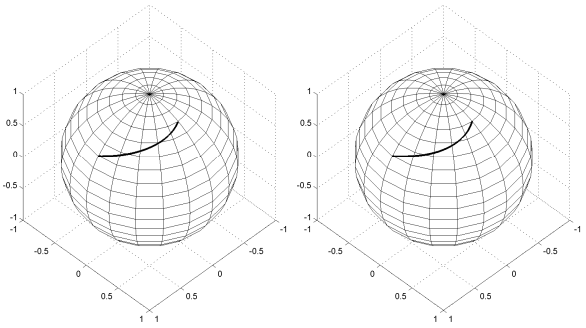

(a) A = 0.5 (b) A = 1

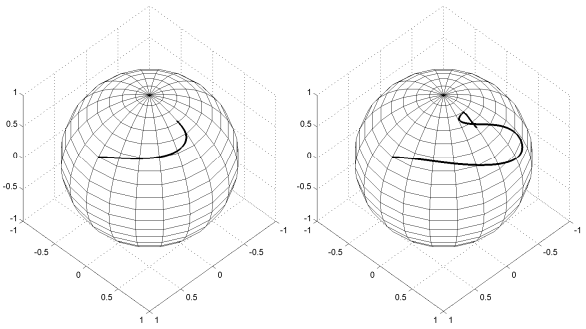

(c) A = 5 (d) A =50

Fig. 4: Head movement to an arbitrary head position, under the influence of a potential function and a constant friction term. We have chosen $\varepsilon = 0.1$ and $k = 1.0$.

VII. CONCLUSION

We have outlined how motion equations can be derived starting from a suitable Riemannian Metric and writing down the corresponding Euler Lagrange equation. In particular, these metrics are written down for $\mathbf{SO}(3)$ and one of its important submanifold **DOND**. Writing down the corresponding Euler Lagrange equation is a standard exercise in Classical Mechanics (see Abraham and Marsden [1]). In this study, head movements have been actuated by a suitable choice of a potential function. The oscillatory response of the head in Fig. 2 has been damped by adding a damping term. An important observation of this paper is in Fig. 5, wherein we show that, within the class of head actuation considered in this paper, for larger values of ε, the transition times between two headings are shortened. This would indicate that for quick head movement using a judicious choice of a potential function

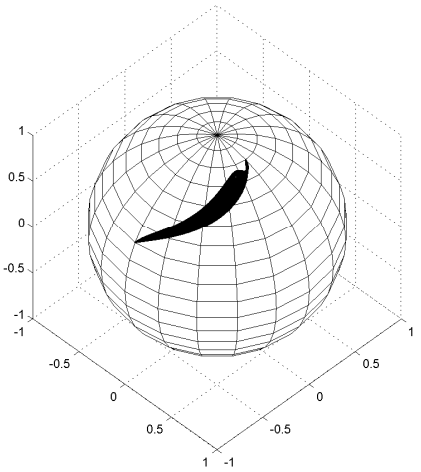

(a) Trajectories of the head direction as ε varies from 0 to 1.

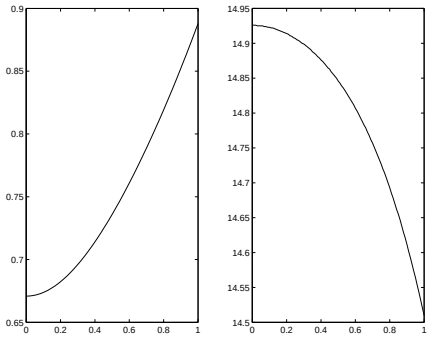

(b) (Left) Distance as a function of ε. (Right) Time as a function of ε

Fig. 5: For increasing values of ε, the head moves a longer distance in a shorter time.

It Would Pay to Slightly Tilt Your Head.

REFERENCES

[1] Abraham, R., Marsden, J. E., *Foundations of Mechanics*, AMS Chelsea Publishing, American Mathematical Society, Providence, Rhode Island, 1978.

[2] Angelaki, D., "Eyes on Target: What Neurons Must Do For The Vestibuloocular Reflex During Linear Motion", *J. Neurophysiol.*, vol. 92, pp. 20–35, 2004.

[3] Angelaki, D. and Hess, B. J. M., "Control of Eye Orientation: Where Does the Brain's Role End and the Muscle's Begin", Review Article, *European J. of Neuroscience*, vol. 19, pp. 1–10, 2004.

[4] Boothby, W. M., *An Introduction to Differentiable Manifolds and Riemannian Geometry*, CA: Academic-Press, 1986.

[5] Bullo, F. and Lewis, A. D., *Geometric Control of Mechanical Systems*, Springer-Verlag, 2004.

[6] Crawford, J. D., Ceylan, M. Z., Klier, E. M. and Guitton, D., "Three Dimensional Eye-Head Coordination During Gaze Saccades in the Primate", *J. Neurophysiol.*, vol. 81, pp. 1760–1782, 1999.

[7] Crawford, J. D., Martinez-Trujillo, J. C. and Klier, E. M., "Neural Control of Three-Dimensional Eye and Head Movements", *Current Opinion in Neurobiology*, vol. 13(6), pp. 655–662, Dec. 2003.

[8] Donders, F. C., "Beiträge zur Lehre von den Bewegungen des menschlichen Auges", *Holländische Beiträge zu den anatomischen und physiologischen Wissenschaften*, vol. 1, pp. 104–145, 1848. Press, 1996.

[9] Ghosh, B. K. and Wijayasinghe, I. B., "Dynamic Control of Human Eye on Head System", *Proc. of the* 29^{th} *Chinese Control Conference,* $29^{th} - 31^{st}$, July, 2010*, Beijing, China*, (to appear).

[10] Ghosh, B. K. and Wijayasinghe, I. B., "Geometric Control of Human Eye Under Head Fixed and Head Free Constraints", *IEEE Transactions in Automatic Control*, (to be submitted).

[11] Glasauer, S., "Current Models of the Ocular Motor System", *Neuro-Ophthalmology, Dev. Ophthalmology*, Basel, Karger, vol. 40, pp. 158–174, 2007.

[12] von Helmholtz, H., *Handbuch der Physiologischen Optik.* Leipzig: Vos., 1866; vol 3, 3^{rd} ed, Leopold Voss, Hamburg & Leipzig, 1910.

[13] Klier, E. M., Wang, H. and Crawford, D., "Neural Mechanisms of Three-Dimensional Eye and Head Movements", *Ann. N. Y. Acad. Sci.*, vol. 956, pp. 512–514, 2002.

[14] Lehnen, N., Buttner, U. and Glasauer, S., "Vestibular Guidance of Active Head Movements", *Exp. Brain Res.*, vol. 194, pp. 495–503, 2009.

[15] Listing, Johann Benedict, *Beitrge zur physiologischen Optik.* Göttinger Studien, Vandenhoeck und Ruprecht, Göttingen, 1845.

[16] Martin, C. and Schovanec, L., "Muscle Mechanics and Dynamics of Ocular Motion", *J. of Mathematical Systems, Estimation and Control*, vol. 8, pp. 1–15, 1998.

[17] Medendorp, W. P., Gisbergen, J. A. M. Van., Horstink, M. W. I. M. and Gielen, C. C. A. M., "Donders' Law in Torticollis", *J. Neurophysiology*, vol. 82, pp. 2833–2838, 1999.

[18] Miller, J. and Robinson, D., "A Model of the Mechanics of Binocular Alignment", *Computers and Biomedical Research*, vol. 17, pp. 436–470, 1984.

[19] Murray, R. M., "Nonlinear Control of Mechanical Systems: A Lagrangian Perspective", *Annu. Rev. Control*, vol. 21, pp. 31–45, 1997.

[20] Polpitiya, A. D., Dayawansa, W. P., Martin, C. F., and Ghosh, B. K., "Geometry and Control of Human Eye Movements", *IEEE Transactions in Automatic Control*, vol. 52, no. 2, pp. 170–180, Feb. 2007.

[21] Quaia, C. and Optican, L., "Commutative Saccadic Generator is Sufficient to Control a 3D Ocular Plant with Pulleys", *J. Neurophysiol.*, vol. 79, pp. 3197–3215, 1998.

[22] Radau, P., Tweed, D. and Vilis, T., "Three Dimensional Eye head and Chest Orientations Following Large Gaze Shifts and the Underlying Neural Strategies", *J. Neurophysiol.*, vol. 72, pp. 2840–2852, 1994.

[23] Raphan, T., "Modeling Control of Eye Orientation in Three Dimension – Role of Muscle Pulleys in Determining Saccadic Trajectory", *J. Physiol.*, vol. 79, pp. 2653–2667, 1998.

[24] Robinson, D., "The Mechanics of Human Saccadic Eye Movement", *J. Physiol.*, vol. 174, pp. 245–264, 1964.

[25] Ruete, C. G. T., *Das Ophthalmotrop, dessen Bau und Gebrauch*, Göttinger Studien. Göttingen, Vandenhoeck und Ruprecht, 1845.

[26] Ruete, C. G. T., *Lehrbuch der Ophthalmologie*, Braunschweig, 1846; 2nd edition, 1853.

[27] Tweed, D. and Villis, T., "Geometric Relations of Eye Position and Velocity Vectors During Saccades ", *Vision Res.*, vol. 30, pp. 111–127, 1990.

[28] Tweed, D., "Three Dimensional Model of the human Eye-Head Saccadic System", *J. Neurophysiology*, vol. 77, pp. 654–666, 1997.

[29] Tweed, D., Haslwanter, T. and Fetter, M., "Optimizing Gaze Control in Three Dimensions", *Science*, vol. 281(28), pp. 1363–1365, Aug., 1998.